Nuclear Fusion in Condensed Matter

V.ROMODANOV, V.SAVIN, Ya.SKURATNIK*, Yu.TIMOFEEV

142109, Podolsk, Moscow Region, Zheleznodorozhnaya 24, RI of SPA LUTCH. Fax. 095-137-9384
*Moscow, SRPCI named after Karpov

ABSTRACT

On the basis of the analysis of the energy loss by a fast particle in a solid it is supposed that the most probable energy range for the reactions of nuclear fusion in condensed media is in the range of the reduced energy of the interacting particles from ε_0 to ε_2 ($\sim$(10-400)$\cdot$1.6$\cdot$10^{-19} J for D-D reactions).

The tritium generation rate has increased by four orders of magnitude, while increasing the specific power by a factor of four, and it has reached the value of 10^9 atom$\cdot$s^{-1} when the neutron-to-tritium yield ratio is in the range from 10^{-7} to 10^{-9}.

The possibility of performing the reactions of nuclear fusion in condensed media between deuterium and target atoms at low energies is shown on the basis of the high-energy β-radiation recording, the isotopic target composition change and the radiography results.

1. Introduction

Investigation of nuclear fusion in condensed matter (NFCM) was performed according to the following stages: from groundless hopes to systematic search for some effects published before and to detection of the conditions under which these effects take place.

We were the first to use deuterium ion bombardment of different targets out of the powerful glow discharge medium for systematic investigation of the NFCM effects /1-3/.

The aim of this work is to determine the optimal range of the NFCM energies when bombarding different

FRONTIERS OF COLD FUSION

targets with accelerated deuterium ions and to define the neutron-to-tritium yield ratio more exactly.

2. Model concepts

As a basis of the model of deuterons interaction in a solid it is supposed that the fusion reaction between them will be possible when two deuterons and one atom of the target matrix hit one intersite cell. In this case the reaction must be threshold (the energy of displacement of the crystalline matrix atom is $(10-30)\cdot 1.6\cdot 10^{-19}$ J for different materials) and the collisions of the deuterons between each other and the target atoms are studied in the energy range exceeding the threshold one on the basis of the analysis of the energy lost by fast particles in a solid. This is possible at be having correlation between local (nuclear) and integral (atoms) collisions. Such an analysis is developed rather well for other fields of physics, in particular, for studying solid surface sputtering /4/.

In terms of this analysis we supposed that one of the possible energy intervals for nuclear fusion is defined by the ratio of the elastic (nuclear) and nonelastic (electronic) losses when accelerated particles move in a solid.

The energy transfer from the moving ion to the target atoms as a result of the elastic collisions is called nuclear deceleration and as a result of the nonelastic collisions - electronic deceleration. The dimensionless values of the current coordinate R and energy E are used in the theory of ion path in amorphous substances, developed by J.Lindhard, M.Scharff, H.E.Schioett (LSS) /5/.

$$\varepsilon \equiv E \left(\frac{M_2}{M_1+M_2} \right) / \frac{Z_1 \cdot Z_2 \cdot e^2}{a_{TF}} ,$$

$$\rho \equiv R \left(\frac{M_1 \cdot M_2}{(M_1+M_2)^2} \right) \cdot 4\pi a_{TF}^2$$

where R - energy of the incident particle; M_1 and M_2 - masses of the incident particle and the target atoms, respectively; Z_1 and Z_2 - atomic numbers; a_{TF} - Thomas-Fermi shielding distance; e - electron charge.

The total average energy losses are equal to the sum of the losses caused by the nuclear and electronic deceleration:

$$-\frac{dE}{dR} = N\,/S_n(E) + S_e(E)/,$$

where $S_n(E)$ - nuclear decelerative ability; N - avera-

ge number of atoms per target volume unit: $S_e(E)$ - electronic decelerative ability.

Only one universal curve which is supposed to be true for all ion-target combinations can be found by varying $(d\varepsilon/d\rho)_n$ depending on ε (fig.1). The peak of the nuclear loss curve corresponds to $\varepsilon_1 \simeq 0.35$.

The specific electronic losses are the following:

$$\left(-\frac{d\varepsilon}{d\rho}\right)_e = K_e \cdot \varepsilon^{0.5}$$

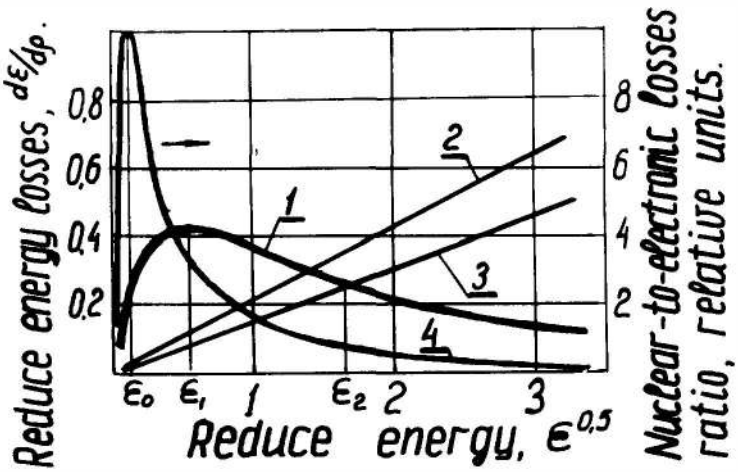

Fig. 1. Reduced energy losses $d\varepsilon/d\rho$ versus the reduced energy $\varepsilon^{0.5}$

1 - nuclear (elastic) losses, Thomas-Fermi potential; 2 - electronic losses, K_e=0.2; 3 - electronic losses, K_e=0.15; 4 - nuclear - to - electronic losses ratio (K_e=0.2)

The values K_e for most of the deuterium ion - target combinations is in the range 0.1-3.

For deuterium ions bombarding the condensed deuterium the calculated energy of the maximum nuclear losses corresponds to $30 \cdot 1.6 \cdot 10^{-19}$ J and the maximum ratio of nuclear-to-electronic losses according to P.Sigmund /4/ corresponds to the energy $7 \cdot 1.6 \cdot 10^{-19}$ J.

Thus, the maximum of the absorbed energy of the atom collisions is near the nuclear loss maximum corresponding to the energy ε_1 (see fig. 1) and the energy, absorbed when the particles collide, decreases considerably after the electronic losses exceed the nuclear ones, that corresponds to the energy ε_2 (see fig. 1). In view of the above-mentioned we consider that the most probable range of the NFCM energy is from ε_0 up to ε_2, the calculated values of which for some

ion-target combinations are given in Table 1. In this Table one can see that depending on the used ion-target combination of the interacting elements the energy of the maximum nuclear losses can reach a few hundreds of keV. According to the accepted model the nuclear interaction efficiency for moderate ion fluxes when using accelerated ions, can be estimated by the coefficient similar to the sputtering one. We called it the nuclear interaction coefficient which is the ratio of the amount of one of the nuclear reaction products to the number of the ions incident on the target made of the given material:

$$Y_n = \frac{\text{number of formed particles}}{\text{number of incident ions}}$$

Table 1

Characteristic energy values for different combinations of deuterium interaction with elements

Target	K_e	E_o, eV	E_1, eV	E_2, eV
^{2}H	0.09	7	30	370
^{7}Li	0.18	9	70	470
^{9}Be	0.21	10	100	510
^{11}B	0.24	11	130	610
^{23}Na	0.42	14	310	730
^{24}Mg	0.43	15	350	760
^{27}Al	0.48	15	380	980
^{45}Sc	0.73	18	700	720
^{48}Ti	0.77	18.1	740	740
^{51}V	0.81	18.4	780	670
^{89}Y	1.29	22.3	1530	400
^{91}Zr	1.31	22.5	1580	410
^{93}Nb	1.34	22.7	1630	360
^{232}Th	2.93	39	4520	-

The reaction product yield isn't supposed to depend on the density of the bombarding ion flux.

3. Experimental procedure and results

The plant construction and the experimental procedure of recording neutrons and tritium, which are

brought about when bombarding different targets by accelerated deuterium ions, are deseribed in /2/. The discharge unit of the plant is designed according to the diode circuit of the direct current in which the specimen of the cathode is bombarded by the deuterium ions out of the glow discharge plasma when the positive potential is applied to the anode. The lamellar specimens ~130 mm in diameter and from 0.05 up to 1 mm thick, located on the cooled substrate, as well as the cylindrical and rod ones having 5-20 mm in diameter were studied. The deuterium containing protium (up to 5% in atomic fractions) and tritium (up to $(5-7)\cdot10^{-10}$%) and having the pressure within $10-5\cdot10^{4}$ Pa was used as a gas which generated plasma. The ion energy changed within $(20-10^{4})\cdot1.6\cdot10^{-19}$ J both at the expense of the supply voltage and at the expense of changing the plasma generating gas pressure in the plant chamber. The current density was $25-5\cdot10^{3}$ A·m^{-2} and the speciment temperature was from 300 up to 2100K.

The thermal effects of the fusion reactions were determined by two methods at the experimental unit the diagram of which is shown in fig.2. The heat flow obtained as a result of the supposed nuclear fusion reaction was determined by measuring the temperature difference both in the measurement section at the temperatures up to 1000K and along the both sides of the weld at the temperatures higher than 1300K by the pyrometer OMP-54. The accuracy of such measurements didn't exceed ±50%.

Some results of measuring the tritium fluxes and their neutron ratio, when irradiating a number of elements by the accelerated deuterium ions out of the glow discharge plasma, are given in Table 2. In this table one can see that β-activity of the plasma-generating gas considerably exceeds the initial one after the gas exposure in the plant chamber under the above-mentioned experimental conditions. The most stable results on tritium generation were obtained when bombarding the erbium and molybdenum specimens by the accelerated deuterium ions and the maximum results were obtained for the niobium specimens. The recorded tritium fluxes were within $10^{5}-10^{9}$ atom·s^{-1}. The unexpectedly high rate of tritium generation (~10^{8} atom·s^{-1}) was obtained when bombarding a material which doesn't generate any hydrides under normal conditions, e.g. when bombarding tungsten.

The recorded neutron-to-tritium flux ratio is from 10^{-3} up to 10^{-9} and mainly depends on the recorded tritium fluxes. Therefore, one shouldn't consider it final.

The tritium content in the near-surface layer of

the specimens after the ion bombardment didn't correspond to its content in gas. The analysis made in the flow detector according to the procedure of measuring the electron spectrum depending on the energy (MSU /6/) showed that after the deuteri m ion bombardment

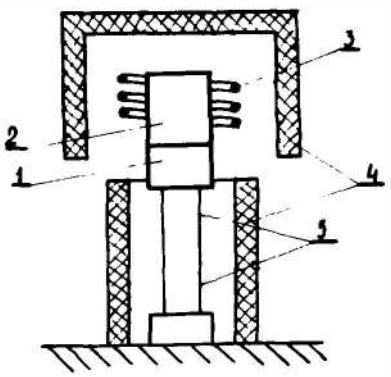

Fig. 2. The diagram of the device for thermal effect determination

1 - molybdenum specimen base; 2 - a part of the hydride-generating material; 3 - anode; 4 - ceramic insulators; 5 - thermocouples

the averaged tritium concentration in the near-surface niobium layer was 10^{7}-10^{8} atom·s^{-2} and in the near-surface tungsten layer (the tritium concentration in gas phase was less by an order of magnitude) the tritium concentration was within $5\cdot10^{9}$-$5\cdot10^{10}$ atom·cm^{-2} The energy spectrum of the radiation from the niobium surface (fig.3) is close to the curve of the tritium β-decay.

The nuclear interaction coefficient when generating tritium (specific flux) versus the bombarding deuteron energy is shown in fig. 4. The feature of th dependence is a threshold availability in the range $70\text{-}150\cdot1.6\cdot10^{-19}$ J. When increasing the bombarding io energy for the materials under investigation, the nuclear interaction coefficient has increased from 10^{-14}

Table 2

Ratio of neutron and tritium fluxes when irradiating a number of materials by deuterium ions

Material	Process parameters			Background, pulse/100 s	Reduced activity in view of background, Bc/ml	Ratio of deuterium activities after and before experiments	Tritium atom flux, atom/s	Nuclear interaction coefficient, atom/ion	Neutron-to-tritium flux ratio	
	E, eV	T, K	τ, h						min	max
D_2	-	-	-	240	130	-	-	-	-	-
Y	40	1170	80	210	290	2.2	$1.2\cdot10^{5}$	$4.1\cdot10^{-15}$	$8.5\cdot10^{-6}$	$1.7\cdot10^{-3}$
Y	80	1270	23	250	$1.2\cdot10^{3}$	9.2	$4.5\cdot10^{6}$	$1.6\cdot10^{-12}$	$2.2\cdot10^{-7}$	$4.4\cdot10^{-5}$
Mo	125	1470	10	150	$6\cdot10^{3}$	46	$4.5\cdot10^{6}$	$9.2\cdot10^{-12}$	$2.2\cdot10^{-7}$	$4.4\cdot10^{-5}$
Mo	100	970	10	170	$1.6\cdot10^{3}$	12.3	$1.8\cdot10^{7}$	$5.9\cdot10^{-12}$	$5.5\cdot10^{-8}$	$1.1\cdot10^{-5}$
Nb	75	1170	162	230	$4.7\cdot10^{4}$	$3.6\cdot10^{2}$	10^{7}	$3.8\cdot10^{-13}$	10^{-7}	$2\cdot10^{-5}$
Nb	80	1170	60	700	$3\cdot10^{6}$	$2.3\cdot10^{4}$	$1.7\cdot10^{9}$	$6.8\cdot10^{-11}$	$0.6\cdot10^{-9}$	$1.8\cdot10^{-7}$
Nb	100	1670	8	240	$5.5\cdot10^{4}$	$4.2\cdot10^{2}$	$0.9\cdot10^{9}$	$1.2\cdot10^{-10}$	$1.1\cdot10^{-9}$	$2.2\cdot10^{-7}$
Er	50	1070	140	460	$1.2\cdot10^{3}$	9.6	$3.1\cdot10^{5}$	$9.9\cdot10^{-15}$	$3.2\cdot10^{-6}$	$6.4\cdot10^{-4}$
Er	70	1270	6	530	$8.9\cdot10^{2}$	6.8	$1.5\cdot10^{7}$	$3.2\cdot10^{-12}$	$6.7\cdot10^{-8}$	$1.3\cdot10^{-5}$
Ta	70	1570	110	350	$3.1\cdot10^{3}$	23.5	$9.6\cdot10^{5}$	$3.6\cdot10^{-14}$	$1.1\cdot10^{-6}$	$2.1\cdot10^{-4}$
Ta	90	1670	5	180	$1.6\cdot10^{3}$	12.3	$3.4\cdot10^{7}$	$7.3\cdot10^{-12}$	$2.9\cdot10^{-8}$	$5.9\cdot10^{-6}$
W	70	1500	115	600	$8.5\cdot10^{5}$	$6.5\cdot10^{3}$	$2.5\cdot10^{8}$	$9.1\cdot10^{-12}$	$4\cdot10^{-9}$	$8\cdot10^{-7}$
W	110	1670	10	760	$1.3\cdot10^{4}$	10^{2}	$1.7\cdot10^{8}$	$2.5\cdot10^{-11}$	$5.8\cdot10^{-9}$	$1.2\cdot10^{-6}$

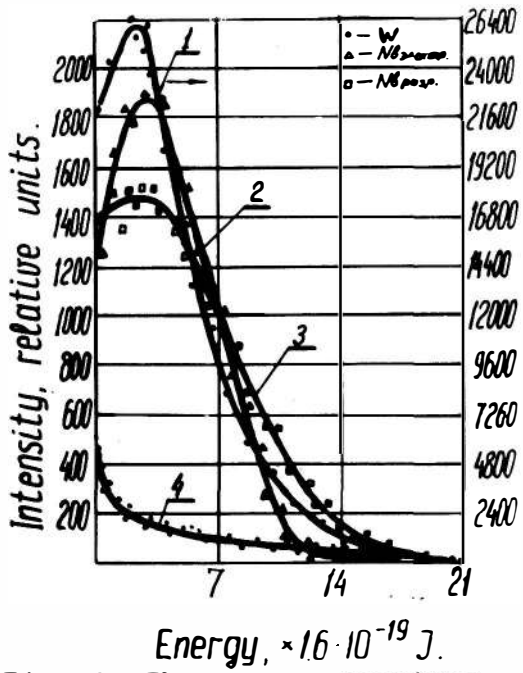

Fig. 3. The energy spectrum of β-radiation on surfaces of different materials

1 - tungsten after ion bombardment ($E=70 \cdot 1.6 \cdot 10^{-19}$ J, T=1500K, τ=115 h); 2 - niobium after having been saturated with tritium by means of electrolysis; 3 -niobium after ion bombardment ($E=75 \cdot 1.6 \cdot 10^{-19}$J, T=1170K, τ=162 h); 4 - starting tungsten

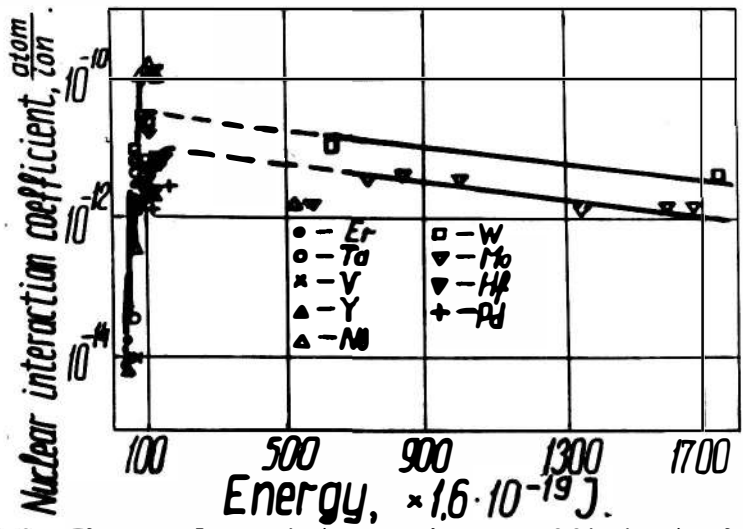

Fig.4. The nuclear interaction coefficient when generating tritium versus the energy of the bombarding deuterium ions for different target materials

-10^{-13} atom·ion^{-1} up to $10^{-11} - 10^{-10}$ atom·ion^{-1}. The average value of the threshold energy is by an arder of magnitude higher than the $\mathcal{E}_0$ estimation made according to Sigmund and 2-5 times higher than the displacement threshold ((10-30)·1.6·10^{-19} J). One failed to determine explicit the energy corresponding to the maximum values of Y_n. It is supposed to be in the range (200-400)·1.6·10^{-19} J. This energy is almost by an order of magnitude higher than $\mathcal{E}_1$(30·1.6·10^{-19} J) for the deuterium target, that may be caused by the metallic matrix effect. The obtained, rather low values of the energies of the maximum nuclear interaction can be also connected with the features of the experimental procedure, according to which the experiments with the deuteron energies exceeding 500·1.6·10^{-19} J were performed at lower pressures of the plasma-generating gas and, therebefore, at lower deuterium concentrations in a metal.

Thus, all the reproduced and reliable NFCM results can be most effectively obtained in the range of the energies of the bombarding deuterium ions from 100·1.6·10^{-19} J up to 500·1.6·10^{-19}J.

The availability of the radiation from the surface is also verified by the specimen radiography (fig.5). The radiogram with the total exposure of two emulsion layers 0.02-0.03 mm thick, located on the both

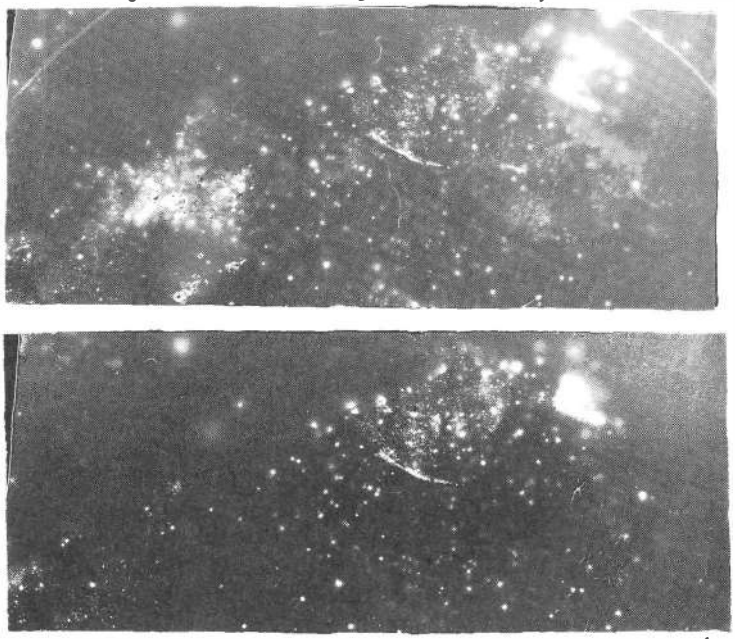

a

b

Fig.5. The yttrium specimen radiogram (T=1170K, τ =80 h):
a-starting film; b-the emulsion layer adjacent to the cpecimen is removed

sides of the triacetate base 0.16-0.18 mm thick (see fig.5a),as well as with the exposure of the same film but with the removed emulsion layer directly adjacent to the specimen (see fig.5b) is shown for yttrium. One can see that the film is pointwise exposed from the outside, though the number of the points is less. The outer emulsion layer was probably exposed at the expense of availability of the particles or radiation having a higher penetration rather than at the expense of the radiation caused by the tritium β-decay.

The recording of β-radiation from the yttrium specimen surface, with the gas detector the thereshold energy 160 keV and the efficiency 60%, allowed to record the count level excess over the background up to 12% and to measure the time response of the decay (Table 3).

Table 3

β-radiation pulse count rate versus time for yttrium after ion bombardment ($E=110 \cdot 1.6 \cdot 10^{-19}$ J, $I=0.3$ A, $\tau=24$ h)

Time (counting origin-bombardment finish), h	1	7	31	79
Counting rate (minus background), pulse$\cdot s^{-1}$	0.12 ± 0.10	0.055 ± 0.048	0.031 ± 0.021	0.015 ± 0.0

According to the estimation the $^{90}_{39}Y$ generation rate is equal to $1 \cdot 10^{-1}$ atom$\cdot s^{-1}$, that accounts for 10^{-6} of the tritium generation rate.

The results of the thermal balance measurement (fig.6) are compared with the calculated temperature difference for the total power 1, for the supposedly maximum power dissipating at the specimen of the cathod 3 and accounting for 50% of the total one, for the minimun power dissipating at the specimen of the cathode 4 and accounting for 30% of the total one and for the experimentally measured one 2. In comparison with the estimations of the heat coming to the specimen of the cathode the maximum excess for the total applied power 70 W at the temperature $\sim$ 600K was from 30% up to 100% supposedly as a result of the nuclear fusion reaction.

The tungsten and niobium specimens were investigated before and after the deuterium ion bombardment at the device MS-720IM by the secindary ion mass-spectrometry (SIMS) method. The ratios of the intensities of

the mass peaks of the specimens under study in the initial state and after the ion bombardment are given in Table 4.

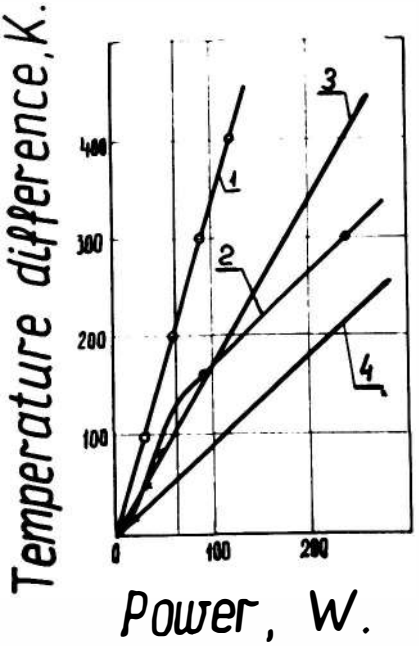

Fig. 6. The temperature difference versus the applied power

1 - calculational dependence for the total power; 2 - experimental dependence; 3 - estimation for the maximum power dissipated at the cathode; 4 - estimation for the minimum power dissipated at the anode

Table 4

Change in the ratio of the ion current of the elements to that of the light isotope of the specimen material as a result of the deuterium ion bombardment

Mass, AMU	Ion current ratio			
	Initial niobium	Niobium after bombardment	Initial tungsten	Tungsten after bombardment
93	1	1	-	-
94	0.07	0.7	-	-
182	-	-	1	1
183	-	-	0.69	0.76
184	-	-	1.25	1.16
185	-	-	0.16	0.24
186	-	-	0.01	0.86
187	-	-	0.16	0.18

The peak of the 94^{th} mass in the niobium-spectrum has considerably increased after the deuterium ion bombardment. In this case the presence of the 95^{th} mass (NbD) hasn't been detected.

Thus, the emulsion exposure from the outside during the radiographic experiments, availability of the high-energy β-radiation as well as the isotopic composition change registered by the SIMS mean that at relatively low energies the following NFCM reactions are possible not only between the deuterium atoms but also between the deuterium and target atoms:

$$^{93}_{41}Nb + ^{2}_{1}H \longrightarrow ^{94}_{41}Nb + ^{1}_{1}H + 5\ MeV.$$

4. Conclusion

1. The threshold character of the dependence of the nuclear interaction rate on the energy of the bombarding deuterium ions has been detected in the NFCM reactions. When increasing the ion energy by a factor of two (from $50 \cdot 1.6 \cdot 10^{-19}$ J up to $100 \cdot 1.6 \cdot 10^{-19}$ J), the tritium generation rate has increased by 2-4 orders of magnitude.

2. The new energy range ($(100\text{-}500) \cdot 1.6 \cdot 10^{-19}$J) allowing to increase the reproducibility and reliability of the experiments was determined for the NFCM investigation.

3. It is shown that the dependence of the nuclear interaction coefficients on the atomic number of the target element isn't monotonic. The highest values of the nuclear interaction coefficient were obtained for niobium ($\sim 10^{-10}$ atom$\cdot$ion^{-1}) and for tungsten and hafnium ($\sim 10^{-11}$ atom$\cdot$ion^{-1}).

4. The tritium fluxes reaching the value of 10^{9} atom$\cdot$s^{-1} and the neutron fluxes close to the background ones don't allow yet to consider the neutron-to-tritium flux ratio at the level 10^{-9}-10^{-7} to be the final value.

5. The calorimetric measurements shouldn't be interpreted unambiguously yet because of the low sensitivity and accuracy of the experiments. The subsequent increase in the measurement accuracy and matching between the generated heat and the other NFCM products is required.

6. The data on radiography, high-energy β-radiation recording as well as on changing in the isotopic composition of the target show that at relatively low energies the NFCM reactions between the deuterium and target atoms, which are similar to the deuterium-deuterium reactions, are possible.

Acknowledgement

The authors are grateful to Dr.V.A.Modin for his assistance in the experimental plant development, Dr. S.G.Korneev for the high-energy γ-and β-activity measurements as well as Prof. R.N.Kuzmin and Dr. P.O.Revokatov for investigating tritium on the specimen surface.

References

1. V.A.Romodanov, V.I.Savin, M.V.Shakhurin, V.T.Chernyavsky, A.E.Pustovit.
Nuclear fusion in a solid. -
International Conference on Radiative Material Science. Alushta, May 22-25, 1990. Poster report 1-100. Theses of the reports. Kharkov, 1990, 1-95, part II, p. 80 (in Russian).
2. V.A.Romodanov, V.I.Savin, M.V.Shakhurin, V.T.Chernyavsky, A.E.Pustovit. Nuclear fusion in a solid.- Zhurnal tekhnicheskoy fiziki, 1991, volume 61, issue 5, p. 122-125 (in Russian).
3. V.A.Romodanov, V.I.Savin, Ya.B.Skuratnik, Yu.M.Timofeev.
Reactions of nuclear fusion in condensed matter.- Voprosy atomnoj nauki i tekhniki. Ser.: Radiation damage physics and radiation technology. 1992, Issue 1 (58), 2 (5-), p. 73-82. (in Russian).
4. Sputtering by Particle Bombardment I.
Physical sputtering of single-element solids. -
Edited by Behrisch.
Springer - Verlag.
Berlin-Heidelberg-New York, 1981.
5. D.Palmer. Ion implantation progress. -
In: Ion implantation into semiconductors and other materials. Edited by V.S.Vavilov. Novosti fiziki tvyordogo tela.
Issue 10. Moscow, Mir, 1980- 330 p. (in Russian).
6. R.N.Kuz'min, E.M.Sakharov, B.N.Shvilkin, A.P.Kuprin, P.O.Revokatov.
Observation of fast neutrons and tritium during electrolysis of heavy water. -
Institute for Nuclear Physics, Moscow State University. Moscow, USSR. Preprint - 90 - 58%204, 1990, - 12 p.